High-Performance β-Ga_2O_3 Schottky barrier diodes and Metal-Semiconductor Field-Effect Transistors on a Non-Delta-Doped High Doping Level Epitaxial layer

Qihao Zhang[a], Jiangwei Liu[b], Chunming Tu[a], Dongyuan Zhai[a, *], Min He[a], Jiwu Lu[a, *]

[a] College of Electrical and Information Engineering, Hunan University, Changsha, Hunan 410082, People's Republic of China
[b] Research Center for Functional Materials, National Institute for Materials Science, Ibaraki 305-0044, Japan
Email: jiwu_lu@hnu.edu.cn and dyzhai@hnu.edu.cn

Abstract

High-performance β-Ga_2O_3-based Schottky barrier diodes (SBDs) and metal-semiconductor field-effect transistors (MESFETs) are fabricated on a non-delta-doped high doping level (>10^{18} cm^{-3}) epitaxial wafer. Their electrical properties and stabilities after annealing at 200~400 °C are investigated. The ON/OFF ratios for all the SBDs are over 10^8. The ideality factors and Schottky barrier heights for the Au/β-Ga_2O_3 SBDs with different annealing temperatures range from 1.5 to 2.5 and from 0.8 eV to 1.0 eV, respectively. There are obvious pinch-off and saturation characteristics for the β-Ga_2O_3 MESFETs. The maximum drain current ($I_{D,max}$) for the as-fabricated β-Ga_2O_3 MESFET is 46.8 mA/mm at anode voltage of 2.0 V. They are much higher than the previously reported values of non-delta-doped and nanobelt β-Ga_2O_3 MESFETs. Threshold voltages for the β-Ga_2O_3 MESFETs shift to the negative direction with the increase of annealing temperature. This study is meaningful to push forward the development of β-Ga_2O_3-based electronic devices for practical applications.

Keywords: β-Ga_2O_3, Schottky barrier diode, MESFET, high doping level

1. Introduction

With the development of power electrical techniques, conventional silicon-based power devices have reached theoretical limitations due to the intrinsic properties of silicon [1]. Third-generation semiconductors such as SiC- and GaN-based power devices have made great progress because of their advantages including wide bandgap energies, high carrier mobilities, high electron saturation velocities, and large thermal conductivities [2, 3]. Their remarkable intrinsic properties promise excellent performances in high breakdown voltage, low power-loss, high-frequency, and high-temperature applications. Recently, β-Ga_2O_3 has attracted lots of attention in next-generation electronic devices. Compared with the SiC and GaN, the β-Ga_2O_3 has a larger bandgap energy of ~4.9 eV, a higher theoretical breakdown electric field of ~8.0 MV/cm, and a higher Baliga's figure of merit of 3214 [4]. Additionally, a large-area, low-cost, and high-quality β-Ga_2O_3 single-crystalline wafer has been commercially available [5], which provides powerful supports to fabricate Ga_2O_3-based electronic devices for practical applications such as in space exploration, high-speed rail, and renewable energy power system.

In recent years, the Ga_2O_3-based metal-semiconductor field-effect transistors (MESFETs) [6–11] have been developed greatly. Higashiwaki *et al*. [6] firstly reported Sn-doped β-Ga_2O_3-based MESFETs on a Ga_2O_3 epitaxial layer grown by a molecular beam epitaxy (MBE) technique. Although they showed good operations, the maximum output current ($I_{D,max}$) was not very high (23.9 mA/mm), which possibly resulted from the low doping concentration (7.0 × 10^{17} cm^{-3}) for the β-Ga_2O_3. Dang *et al*. [7] deposited an α-Ga_2O_3 film on sapphire via a mist-chemical vapor deposition technique for fabricating the MESFETs with a PtO_x Schottky gate. Unfortunately, the quality of α-Ga_2O_3 epitaxial layer was poor, which led to the low channel mobility (1.3 cm^2/Vs) and the low $I_{D,max}$ (0.13 mA/mm) for the MESFET. Bae *et al.* [8] and Ma *et al.* [9] exfoliated mechanically the quasi-two-dimensional β-Ga_2O_3 flakes and transferred them on SiO_2/Si substrates to fabricate the MESFETs, respectively. However, the fabrication processes were complicated and the $I_{D,max}$ value

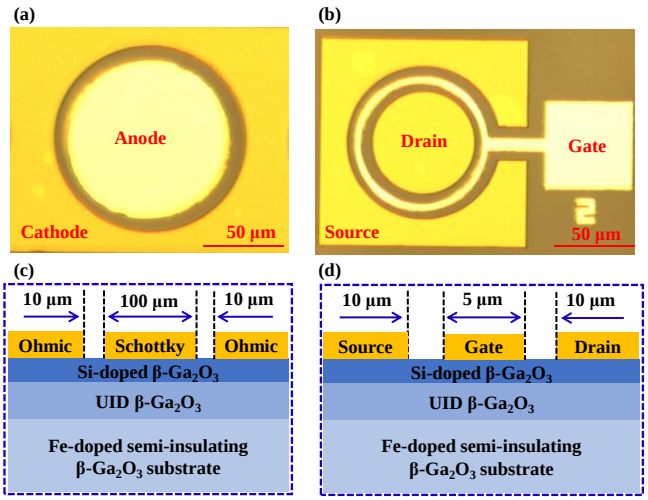

Figure 1. Optical images of the β-Ga_2O_3-based (a) SBD and (b) MESFET, respectively. (c) and (d) cross-sectional views of them, respectively.

(~5.6 mA/mm) was still not satisfactory. Rajan's Group [10−12] made great efforts to grow delta-doped β-Ga_2O_3 epitaxial layers for fabricating the MESFETs. The delta-doping β-Ga_2O_3 was completed in a thin epitaxial layer (~0.2 nm) with an extremely high doping level (~10^{21} cm^{-3}) [12]. There were excellent electrical properties for the delta-doped β-Ga_2O_3-based MESFETs such as a high channel mobilities (95 cm^2/Vs) and a large $I_{D,max}$ value (180 mA/mm) [10, 11]. However, since it needs a high operation technique for the growth of delta-doped β-Ga_2O_3 epitaxial layer, it is a big challenge to promote this technique for wide applications.

In this study, we attempt to fabricate the Schottky barrier diodes (SBDs) and MESFETs on non-delta-doped high doping level (>10^{18} cm^{-3}) β-Ga_2O_3 epitaxial wafer. Their electrical properties will be investigated and compared with the previous reports. The annealing effect on the β-Ga_2O_3-based SBDs and MESFETs will be discussed.

2. Experimental

The β-Ga_2O_3 epitaxial wafer with dimension of 10 mm × 15 mm × 0.5 mm was purchased from Japan Novel Crystal Technology, Inc. A 200 nm-thick Si-doped (010) epitaxial layer was grown on the Fe-doped semi-insulating substrate with a 200 nm-thick unintentionally doped (UID) buffer layer by the MBE technique. The effective donor concentration of the channel layer was extracted to be around 2.0 × 10^{18} cm^{-3} via an electrochemical capacitance-voltage profiling method.

The β-Ga_2O_3 epitaxial wafer was cleaned in acetone, alcohol, and SPM solvent (H_2SO_4 and H_2O_2 mixed solution) for 3, 3, and 5 min, respectively, followed by dipping in deionized water for 15 min. For preparing graphical ohmic contact electrodes, a positive photoresist (AR-P5350) was spin-coated on the sample with a rotation rate of 4000 rpm/min for 1 min. The cathode patterns were formed after the standard lithography process. The Ti/Au (20/80 nm) bilayer were formed by a magnetron sputtering deposition system at the chamber pressure of 5.0 × 10^{-6} Torr [Figs. 1(a, b-ii)]. The deposition rates for Ti and Au were 6.25 nm/min and 100 nm/min, respectively. The sample was thermally annealed at 500 °C for 10 min to form Ohmic contact for the Au/Ti/β-Ga_2O_3.

The anode and gate electrode of Au for both SBD and MESFET were formed by the magnetron sputtering method with the thickness and sputtering rate of 100 nm and 60 nm/min, respectively. In order to investigate thermal stabilities of them, the sample was annealed at 200, 300, and 400 °C in a tube-heated furnace under a N_2 gas atmosphere with an annealing time for each temperature of 10 min. Their electrical properties were measured with a B1500 parameter analyzer and a four-prober system at room temperature.

3. Results and discussion

3.1. Structure of SBD and MESFET

Figures 1(a) and 1(b) show the optical images of the β-Ga_2O_3 SBD and MESFET, respectively. Their cross-sectional views are shown in Figs. 1(c) and 1(d), respectively. The radius and area of the anode for the β-Ga_2O_3 SBD are 50 μm and 7.85 × 10^{-5} cm^{-2}, respectively. The gap spacing between anode and cathode is 10 μm. For the β-Ga_2O_3 MESFET, the gate length (L_G), gap spacing between source and gate electrodes, and gap spacing between gate and drain electrodes are 5, 10, and 10 μm, respectively. As the radius of the drain electrode for the β-Ga_2O_3 MESFET is 50 μm, the gate width (W_G) can be computed to be 0.314 mm.

3.2. Electrical Properties of the Au/β-Ga_2O_3 SBD

Figure 2 shows the current density (J)–voltage (V) characteristic for the β-Ga_2O_3 SBDs. The voltage varies from -5.0 to 10.0 V. Inset figure shows the enlarged curves with the voltage ranging from 9.0 V to 10.0 V. For the as-fabricated SBD, the maximum J (J_{max}) is 905.2 A/cm^2 at the anode voltage of 10.0 V. After the sample is annealed at 200 and 300 °C, the J_{max} values increase gradually to 950.2 and 970.3 A/cm^2, respectively. However, as the annealing temperature enhances to 400 °C, the J_{max} decreases to 717.1 A/cm^2. When the voltage is lower than zero, the J values for the as-fabricated, 300 °C-annealed, and 400 °C-annealed β-Ga_2O_3 SBDs are less than 10^{-5} A/cm^2. Their ON/OFF ratios are in a 10^8 level. That for the 200 °C-annealed one is less than 10^{-8} A/cm^2 with the ON/OFF ratio as large as 1.5 × 10^{11}. Comparing with the as-fabricated Schottky diode, annealing at 200 °C possibly modifies the plasma damage for the β-Ga_2O_3 during the formation of Au electrode by the magnetron sputtering technique [13], which improves the OFF current and ON/OFF ratio for the SBD. As the annealing temperatures increase to 300 and 400 °C, the interfacial qualities of Au/β-Ga_2O_3 are possibly degraded at high-temperature. This is the possible

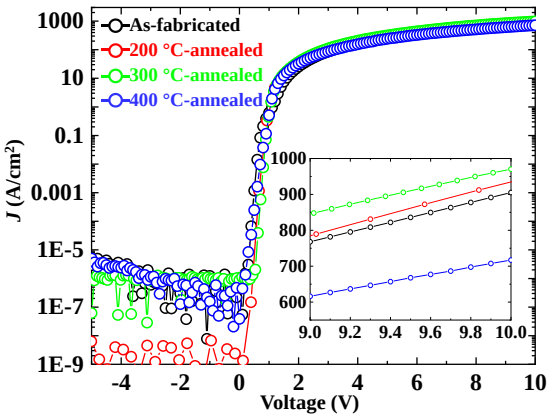

Figure 2. The *J*–*V* characteristics for the β-Ga_2O_3 SBDs. Inset figure shows the enlarged curves at the voltage ranging from 9.0 V to 10.0 V.

Table I Electrical properties of the β-Ga_2O_3 SBDs

	J_{max} (A/cm^2)	ON/OFF	J_s (A/cm^2)	n	Φ_B (eV)
As-fabricated	905.2	3.1×10^8	9.2×10^{-9}	1.6	0.9
200 ºC-annealed	950.2	1.5×10^{11}	1.5×10^{-10}	1.7	1.0
300 ºC-annealed	970.3	7.2×10^8	6.5×10^{-12}	1.5	1.0
400 ºC-annealed	717.1	1.4×10^8	1.4×10^{-7}	2.5	0.8

reason for the lower ON/OFF ratios at higher annealing temperatures.

The measured *J*–*V* characteristics for the Au/β-Ga_2O_3 SBDs follow the thermionic emission (TE) model under V > $3k_BT/q$ condition [14]:

$$J = J_S[\exp(\frac{qV}{nk_BT}) - 1], \quad (1)$$

where the q, n, k_B, and T are the elementary charge (1.6×10^{-19} C), ideality factor, Boltzmann constant (1.38×10^{-23} J/K), and room temperature (300 K), respectively. The J_S is saturation current density, given by:

$$J_S = A^*T^2\exp(\frac{-q\Phi_B}{k_BT}), \quad (2)$$

where the A^* is the effective Richardson constant for β-Ga_2O_3 (41 A/cm^2·K^2) [15]. The Φ_B is the Schottky height of Au/β-Ga_2O_3 interface. By fitting the data in Fig. 3, the J_S, n, and Φ_B can be deduced based on Eq. (1) and Eq. (2), which are summarized in Table I. The n and Φ_B range from 1.5 to 2.5 and from 0.8 eV to 1.0 eV, respectively. The high n values for the Au/β-Ga_2O_3 SBDs are possibly ascribed to the spatial inhomogeneity between Au and β-Ga_2O_3 epitaxial layer. The same phenomena were also observed in other previous reports [16–19]. Additionally, when the Au metals were deposited on other semiconductors such as GaN [20], GaAs [21], and diamond [22], the same situation happened. In the following study, the change of anode and the improvement of the Au/β-Ga_2O_3 interfacial quality would be performed to resolve this issue.

3.3. Electrical Properties of the Au/β-Ga_2O_3 MESFETs

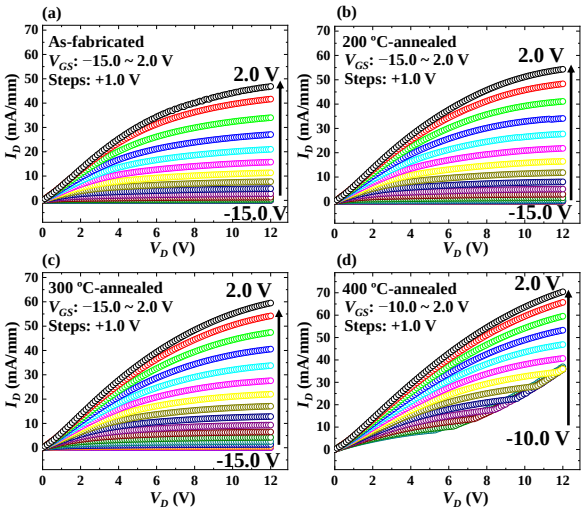

Figure 3. (a)–(d) The I_D–V_D characteristics for the non-annealed and annealed β-Ga_2O_3 MESFETs respectively.

Figures 3(a)–3(d) show drain current versus drain voltage (I_D–V_D) characteristics for the as-fabricated, 200 °C-, 300 °C-, and 400 °C-annealed β-Ga_2O_3 MESFETs, respectively. For the former three MESFETs, gate-to-source voltage (V_{GS}) varies from –15.0 to 2.0 V. That for the 400 °C-annealed one changes from −10.0 to 2.0 V. There are obvious pinch-off and saturation characteristics for the I_D–V_D curves of the as-fabricated, 200 °C-annealed, and 300 °C-annealed β-Ga_2O_3 MESFETs. The 400 °C-annealed one still operates well at V_{GS} = –3.0 ~ 2.0 V. However, when the V_{GS} varies from −10.0 to –4.0 V, its I_D values increase sharply with the change of V_D. One possible explanation is that the Au/β-Ga_2O_3 interface suffers great damage after annealing at 400 °C. The $I_{D,max}$ for the as-fabricated β-Ga_2O_3 MESFET is 46.8 mA/mm at V_{GS} = 2.0 V. Annealing at 200, 300, and 400 °C make it increase to 54.3, 59.5, and 70.5 mA/mm, respectively. The on-resistance (R_{ON}) normalized by the W_G for the β-Ga_2O_3 MESFETs can be obtained by fitting the linear regions of the I_D–V_D characteristics. They are extracted to be 155.7, 148.5, 139.4, and 134.0 Ω mm for the as-fabricated, 200 °C-, 300 °C-, and 400 °C-annealed MESFETs, respectively. Annealing makes the $I_{D,max}$ increase and the R_{ON} decrease for the β-Ga_2O_3 MESFETs. These are possibly caused by the following two factors. On one hand, the R_{ON} of the MESFET is composed of Ohmic contact resistance, surface resistance, and channel resistance, annealing possibly improves the channel resistance under gate region. On the other hand, the modification of Φ_B for the Au/β- Ga_2O_3 interface may affect the $I_{D,max}$ and R_{ON} of the β-Ga_2O_3 MESFETs.

The $\sqrt{I_D}$ as the function of V_{GS} for the as-fabricated and annealed β-Ga_2O_3 MESFETs is shown in Fig. 4(a). By fitting the linear regions of the curves, threshold voltage (V_{TH}) values for them are determined to be −9.5, −11.3, −14.3, and −15.0 V, respectively, which are summarized in Fig. 4 (b). All the β-Ga_2O_3 MESFETs operate in normally-on modes. With the

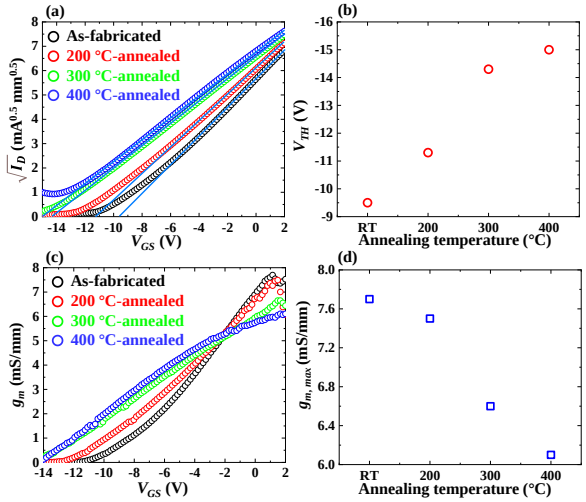

Figure 4. (a) $\sqrt{I_D}$ –V_{GS} and (c) g_m–V_{GS} for the β-Ga_2O_3 MESFETs, respectively, (c) V_{TH} and (d) influence of annealing temperature on $g_{m,max}$ for the β-Ga_2O_3 MESFETs, respectively.

Table II Comparison of our β-Ga_2O_3 MESFET with the previously reported MESFETs [6–9]

	L_G (μm)	$I_{D,max}$ (mA/mm)	V_{TH} (V)	$g_{m,max}$ (mS/mm)
MESFET [6]	4	~ 23.9	~ −15	~ 2.2
MESFET [7]	10	~ 0.13	−0.8	0.5
MESFET [8]	~ 12	~ 2	−7.3	~ 0.2
MESFET [9]	4.2	~ 5.6	−7.1	0.68
MESFET [This work]	5	46.8	−9.5	7.7

increment of annealing temperature, the V_{TH} shifts to the negative direction. The extrinsic transconductance (g_m) as the function of V_{GS} for the β-Ga_2O_3 MESFETs is summarized in Fig. 4(c). For the as-fabricated β-Ga_2O_3 MESFET, the maximum g_m ($g_{m,max}$) is extracted to be 7.7 mS/mm (2.4 mS). They are 7.5, 6.6, and 6.1 mS/mm after the sample annealing at 200, 300 and 400 °C, respectively. Fig. 4(d) summarizes annealing effects on the $g_{m,max}$ for the β-Ga_2O_3 MESFET. The $g_{m,max}$ decreases gradually with the increment of annealing temperature.

4. Conclusion

In summary, the β-Ga_2O_3 SBDs and MESFETs were assembled on the non-delta-doped high doping level epitaxial wafer. The effects of annealing temperature (200~400 °C) on their electrical properties were discussed. The J_{max} and ON/OFF ratio of the as-fabricated SBD reached 905.2 A/cm^2 and 10^8 level, respectively. As the annealing temperature increased to 200 °C, they were improved to be 950.2 A/cm^2 and 1.5×10^{11}, respectively. When the annealing temperature was enhanced to 400 °C, the J_{max} and ON/OFF ratio degraded to 717.1 A/cm^2 and 10^8 level, respectively. The n and Φ_B for the SBDs ranged from 1.5 to 2.5 and from 0.8 eV to 1.0 eV, respectively. The $I_{D,max}$ values for the as-fabricated, 200 °C-, 300 °C-, and 400 °C-annealed β-Ga_2O_3 MESFETs were 46.8, 54.3, 59.5, and 70.5 mA/mm, respectively. They were larger than those of the previously reported non-delta-doped Ga_2O_3-based MESFETs. The absolute V_{TH} values increased gradually with the increment of annealing temperature. The $g_{m,max}$ values for them were 7.7, 7.5, 6.6, and 6.1 mS/mm, respectively, which were also higher than those of the previous reports. The fabrication of high-performance β-Ga_2O_3 SBDs and MESFETs is meaningful to push forward the β-Ga_2O_3-based electronic devices for practical applications.

Declaration of Competing Interest

The authors declare that they have no known competing financial interests or personal relationships that could have appeared to influence the work reported in this paper.

Acknowledgements

This work was supported in part by the National Key R&D Program of China under Grant 2018YFB1201802, in part by the National Natural Science Foundation of China under Grant 51977065, Grant 51807054, and Grant 52177179, and in part by the Science and Technology Innovation Program of Hunan Province, People's Republic of China, under Grant 2019RS1024, and Grant 2020RC5004.

References

[1] B. J. Baliga, The future of power semiconductor device technology, Proc. IEEE. 89 (2001) 822–832. https://doi.org/10.1109/5.931471.

[2] X. She, A. Q. Huang, O. Lucia, B. Ozpineci, Review of Silicon Carbide Power Devices and Their Applications, IEEE Trans. Ind. Electron. 64 (2017) 8193–8205. https://doi.org/10.1109/tie.2017.2652401.

[3] E. A. Jones, F. F. Wang, D. Costinett, Review of Commercial GaN Power Devices and GaN-Based Converter Design Challenges, IEEE Trans. Emerg. Sel. Topics Power Electron. 4 (2016) 707–719. https://doi.org/10.1109/jestpe.2016.2582685.

[4] S. J. Pearton, J. Yang, P. H. Cary, F. Ren, J. Kim, M. J. Tadjer, M. A. Mastro, A review of Ga_2O_3 materials, processing, and devices, Appl. Phys. Rev. 5 (2018) 011301. https://doi.org/10.1063/1.5006941.

[5] A. Kuramata, K. Koshi, S. Watanabe, Y. Yamaoka, T. Masui, S. Yamakoshi, High-quality β-Ga_2O_3 single crystals grown by edge-defined film-fed growth, Jpn. J. Appl. Phys. 55 (2016) 1202A2. https://doi.org/10.7567/jjap.55.1202a2.

[6] M. Higashiwaki, K. Sasaki, A. Kuramata, T. Masui, S. Yamakoshi, Gallium oxide (Ga_2O_3) metal-semiconductor field-effect transistors on single-crystal β-Ga_2O_3 (010) substrates, Appl. Phys. Lett. 100 (2012) 013504. https://doi.org/10.1063/1.3674287.

[7] G. T. Dang, T. Kawaharamura, M. Furuta, M. W. Allen, Mist-CVD Grown Sn-Doped α-Ga_2O_3 MESFETs, IEEE Trans. Electron Devices. 62 (2015) 3640–3644. https://doi.org/10.1109/ted.2015.2477438.

[8] J. Bae, H. W. Kim, I. H. Kang, G. Yang, J. Kim, High breakdown voltage quasi-two-dimensional β-Ga_2O_3 field-effect transistors with a boron nitride field plate, Appl. Phys. Lett. 112 (2018) 122102. https://doi.org/10.1063/1.5018238.

[9] J. Ma, H. J. Cho, J. Heo, S. Kim, G. Yoo, Asymmetric Double-Gate β-Ga_2O_3 Nanomembrane Field-Effect Transistor for Energy-Efficient Power Devices, Adv. Electron. Mater. 5 (2019) 1800938. https://doi.org/10.1002/aelm.201800938.

[10] Z. Xia, C. Joishi, S. Krishnamoorthy, S. Bajaj, Y. Zhang, M. Brenner, S. Lodha, S. Rajan, Delta Doped β-Ga_2O_3 Field Effect Transistors With

Regrown Ohmic Contacts, IEEE Electron Device Lett. 39 (2018) 568–571. https://doi.org/10.1109/led.2018.2805785.
[11] C. Joishi, Z. Xia, J. S. Jamison, S. H. Sohel, R. C. Myers, S. Lodha, S. Rajan, Deep-Recessed β-Ga_2O_3 Delta-Doped Field-Effect Transistors With In Situ Epitaxial Passivation, IEEE Trans. Electron Devices. 67 (2020) 4813–4819. https://doi.org/10.1109/ted.2020.3023679.
[12] S. Krishnamoorthy, Z. Xia, S. Bajaj, M. Brenner, S. Rajan, Delta-doped β-gallium oxide field-effect transistor, Appl. Phys. Express. 10 (2017) 051102. https://doi.org/10.7567/apex.10.051102.
[13] J. Yang, F. Ren, R. Khanna, K. Bevlin, D. Geerpuram, L. -C. Tung, J. Lin, H. Jiang, J. Lee, E. Flitsiyan, L. Chernyak, S. J. Pearton, A. Kuramata, Annealing of dry etch damage in metallized and bare (-201) Ga_2O_3, J. Vac. Sci. Technol. B. 35 (2017) 051201. https://doi.org/10.1116/1.4986300.
[14] S. K. Cheung, N. W. Cheung, Extraction of Schottky diode parameters from forward current-voltage characteristics, Appl. Phys. Lett. 49 (1986) 85–87. https://doi.org/10.1063/1.97359.
[15] K. Sasaki, M. Higashiwaki, A. Kuramata, T. Masui, S. Yamakoshi, Ga_2O_3 Schottky Barrier Diodes Fabricated by Using Single-Crystal β–Ga_2O_3 (010) Substrates, IEEE Electron Device Lett. 34 (2013) 493–495. https://doi.org/10.1109/led.2013.2244057.
[16] X. Z. Liu, C. Yue, C. T. Xia, W. L. Zhang, Characterization of vertical Au/β-Ga_2O_3 single-crystal Schottky photodiodes with MBE-grown high-resistivity epitaxial layer, Chin. Phys. B. 25 (2016) 017201. https://doi.org/10.1088/1674-1056/25/1/017201.
[17] K. Sasaki, M. Higashiwaki, A. Kuramata, T. Masui, S. Yamakoshi, MBE grown Ga_2O_3 and its power device applications, J. Cryst. Growth. 378 (2013) 591–595. https://doi.org/10.1016/j.jcrysgro.2013.02.015.
[18] E. Farzana, Z. Zhang, P. K. Paul, A. R. Arehart, S. A. Ringel, Influence of metal choice on (010) β-Ga_2O_3 Schottky diode properties, Appl. Phys. Lett. 110 (2017) 202102. https://doi.org/10.1063/1.4983610.
[19] L. A. M. Lyle, K. Jiang, E. V. Favela, K. Das, A. Popp, Z. Galazka, G. Wagner, L. M. Porter, Effect of metal contacts on (100) β-Ga_2O_3 Schottky barriers, J. Vac. Sci. Technol. A. 39 (2021) 033202. https://doi.org/10.1116/6.0000877.
[20] B. Roul, T. N. Bhat, M. Kumar, M. K. Rajpalke, A. T. Kalghatgi, S. B. Krupanidhi, Analysis of the temperature-dependent current-voltage characteristics and the barrier-height inhomogeneities of Au/GaN Schottky diodes, Phys. Status Solidi A. 209 (2012) 1575–1578. https://doi.org/10.1002/pssa.201228237.
[21] J. W. P. Hsu, Y. L. Loo, D. V. Lang, J. A. Rogers, Nature of electrical contacts in a metal–molecule–semiconductor system, J. Vac. Sci. Technol. B. 21 (2003) 1928. https://doi.org/10.1116/1.1588641.
[22] T. Teraji, Y. Koide, T. Ito, High-temperature stability of Au/p-type diamond Schottky diode, Phys Status Solidi Rapid Res Lett. 3 (2009) 211–213. https://doi.org/10.1002/pssr.200903151.